

Article

# Elevation Dependence of the Impact of Global Warming on Rainfall Variations in a Tropical Island

Mirindra Finaritra Rabezanahary Tanteliniaina <sup>1</sup>, Jia Chen <sup>2</sup>, Tanveer M. Adyel <sup>3</sup> and Jun Zhai <sup>1,\*</sup>

<sup>1</sup> MOE Key Laboratory of the Three Gorges Reservoir Region's Eco-Environment, Chongqing University, Chongqing 400045, China; mirindra@cqu.edu.cn

<sup>2</sup> MOE Engineering Research Center for Waste Oil Recovery Technology and Equipment, Chongqing Technology and Business University, Chongqing 400067, China; jiachen77@ctbu.edu.cn

<sup>3</sup> Department of Civil Engineering, Monash University, 23 College Walk, Clayton, VIC 3800, Australia; tanveer.adyel@monash.edu

\* Correspondence: zhajun@cqu.edu.cn; Tel.: +86-23-6512-0810 or +86-136-3796-6883; Fax: +86-23-6512-0810

Received: 29 November 2020; Accepted: 17 December 2020; Published: 21 December 2020



**Abstract:** Due to their vulnerability, understanding the impacts of global warming on rainfall is important for a tropical country and islands. This research aimed to assess the impact of global warming on rainfall in Madagascar, using the Mann-Kendall test, continuous wavelet transform, and polynomial regression. The result showed that the annual, seasonal maximum, and minimum temperature increased, while elevation amplified the increase of maximum temperature. Different trends in rainfall were found in the 22 regions of Madagascar but in general, the increasing trend in rainfall was prominent at a higher elevation than lower elevation. The annual rainfall decreased up to  $-5$  mm per year for the regions located below 450 m of altitude while increased up to  $+5$  mm per year above 500 m. We found that the wet becomes wetter with an important increase in rainfall in summer and the increase in temperature influenced the rainfall. The annual rainfall increased with temperature and elevation. However, if the increase in temperature was more than  $0.03$  °C per year, the annual rainfall increased regardless of elevation. The knowledge of the elevation dependence of the impact of warming on rainfall is important for water resources management and climate change adaptation strategies, especially for island nations and African countries.

**Keywords:** global warming; temperature; rainfall; elevation; tropical climate; Madagascar

## 1. Introduction

Since the rise of manmade greenhouse gas emissions, global temperature has continuously increased, with a  $1.07$  °C increase since 1880, and 19 of the 20 warmest years have occurred since 2001, except 1998 [1]. Several studies have demonstrated that global warming impacts the temporal and spatial variation of rainfall and leads to frequent extreme weather [2–5]. In general, global warming intensifies the global hydrological cycle and increases average global precipitation, evaporation, and runoff [6,7]. Change in evaporation leads to more frequent and intense storms, and droughts [2,8]; hence, change in land cover and land use [9]. Moreover, climate change and global warming are also responsible for the degradation of ecosystem services [9]. The impacts of global warming are not evenly distributed among all countries around the world as island nations are more exposed and more affected [4]. Furthermore, due to their weaker economies, the impact of global warming is expected to be more severe in African and tropical countries [2,10–13]. Therefore, adaptation is important [14], especially in African countries. However, to design an effective adaptation strategy, plenty of research is needed. Yet, there has been relatively little work published on the hydro climatological impact of global warming for Africa.

Madagascar is an African island, considered by the World Meteorological Organization to be the third most vulnerable country exposed to global warming [15]. It is located in the Indian Ocean between 12 and 25° latitude south, and the climate of the island is in close and direct relation with the atmospheric circulation of the Indian Ocean [16,17]. The island is a good site and reference for the study of global warming impacts because almost all the climate types in the African continent are present in Madagascar [15,18]. Therefore, research led in Madagascar can be scaled up to the African continent. However, the few studies published concerning climate change in Madagascar found evidence of uneven patterns across the country, and many uncertainties remain on how global warming is affecting the rainfall of the island [15,17]. Researchers have found a correlation between rainfall trend and elevation/altitude [19–22]. The risk of heavy rainfall is generally expected in high-elevation regions [4]. However, the effect of altitude may vary spatially and seasonally [19–23], and very few studies have been published to address the elevation dependence of global warming impacts on rainfall in an African tropical island like Madagascar.

Continuous Wavelet Transform (CWT) is a recent development in signal processing [24,25], and was applied to the 115 years average temperature and rainfall of Madagascar to study the periodicity in the time series. The CWT can provide time-frequency analysis on a time series and is appropriate for hydrological climate studies [24,26]. The non-parametric Mann-Kendall test (MK-test) [27,28] was used to detect the existence of a monotonic trend in the temperature and rainfall data. The MK-test is a robust tool and is effective regardless of outliers and the skewness of the data [24,29–31]. Sen's slope estimator was applied to determine the magnitude of the monotonic trend. Finally, polynomial regression, a non-linear regression, was used to describe the relationship between the elevation, the temperature, and the rainfall. Polynomial regression provides the most flexible curve-fitting relationship between the dependent and independent variables [32].

In this study, the spatio-temporal temperature and rainfall changes along with elevation in Madagascar were investigated, using two different climatic data sets, a long-term data from 1901 to 2015 and a short-term data from 1987 to 2017.

## 2. Materials and Methods

### 2.1. Description of the Study Area

Madagascar is the fourth largest island in the world, located in the southwestern part of the Indian Ocean, just off the South-Eastern edge of the African continent. The country is located at 11°55' S and 25°30' S; 43°10' E and 50°35' E with 592,000 km<sup>2</sup> of total area. Madagascar has a tropical climate, with two distinct seasons: a hot and rainy season from October to March with January as the wettest month, and a dry season from April to September with July as the driest one. Because of its geographical position and the amount of precipitation received each year, Madagascar enjoys five types of climate: arid climate (rainfall < 600 mm per year), Semi-arid climate (rainfall between 600 and 1000 mm per year), tropical savanna climate (rainfall between 1000 and 1500 mm per year), tropical monsoon climate (1500 and 2000 mm per year), and tropical rainforest climate (rainfall > 2000 mm per year) (Figure 1). In terms of topography, the country is characterized by an elevated central plateau running most of the island's length, surrounded by coastal lowlands. The average elevation of the plateau's spine is about 1500 m; the three highest peaks range from 2600 to 2900 m in altitude [33]. Madagascar can be divided into 22 regions and each region owns a meteorological station.

### 2.2. Data Source

For the analysis using CWT, we needed long-term data, so we used historical annual average rainfall and temperature data of 115 years from 1901 to 2017 from the World Bank (<https://climateknowledgeportal.worldbank.org/download-data>). The data were assessed with preliminary analysis by plotting time series and inspecting possible errors and uncertainties. The test results indicated that it was a high-quality data and had no missing values. For the rest of the analysis, we used

31 years (short term data from 1987 to 2017) of quality-controlled regional rainfall and temperature data (maximum and minimum temperature), assembled from the Madagascar National Meteorological and Hydrological Service. No missing data were observed with the short-term datasets. Elevation data were gathered from USGS-NASA (<https://earthexplorer.usgs.gov/>); about 79 digital elevation models (SRTM-DEM) were needed to cover the total area of Madagascar.

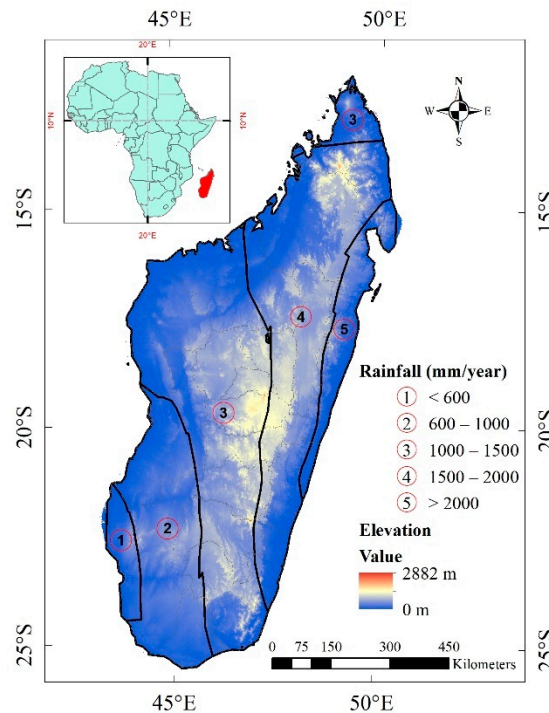


**Figure 1.** Elevation and rainfall map of Madagascar data obtained from Madagascar meteorological and hydrological service and USGS-NASA.

### 2.3. Methods

#### 2.3.1. The MK Test and Sen’s Slope Estimator

The MK test [27,28] was applied to study the rainfall and temperature variations trends. The MK-test is a non-parametric test used to detect a trend in meteorological and hydrological data [34–40]. The WMO recommended it in assessing trends in precipitation and temperature time series. It has the advantage of being effective, regardless of the distribution of the data. In this approach, the differences between each sequential value were calculated to detect a trend. Equation (1) describes the test statistic (S):

$$S = \sum_{k=1}^{n-1} \sum_{j=k+1}^n \text{sgn}(X_j - X_k) \tag{1}$$

where,  $X_i$  is a time-series from  $i = 1, 2, 3, \dots, n - 1$ ,  $X_j$  is another time-series from  $j = i + 1, \dots, n$ ,  $X_j$  is greater than  $X_i$ , and  $n$  is the data set record length.

Each point  $x_i$  is used to reference the point of  $x_j$ , the result recorded as Equation (2):

$$\text{sgn} = \begin{cases} +1 & > (x_j - x_i) \\ 0 & = (x_j - x_i) \\ -1 & < (x_j - x_i) \end{cases} \tag{2}$$

With time-series larger or equal than 10 ( $n \geq 10$ ), the S statistic follows the normal distribution with a mean of  $E(S) = 0$  and the variance ( $\text{Var}(S)$ ) as Equation (3):

$$\text{Var}(S) = \frac{n(n-1)(2n+5) - \sum_{t=i}^m t(t-1)(2t+5)}{18} \quad (3)$$

where  $n$  is the length of the data set and  $t$  is the number of ties with of  $t$ -th value.

Then, the MK-test statistic test  $Z$  can be estimated as Equation (4):

$$Z_c = \begin{cases} \frac{S-1}{\sqrt{\text{Var}(S)}} & S > 0 \\ 0 & S = 0 \\ \frac{S+1}{\sqrt{\text{Var}(S)}} & S < 0 \end{cases} \quad (4)$$

A positive value of  $Z_c$  indicates a positive trend, whereas a negative value represents a negative trend in the time series. At significance level  $\alpha$ , if  $Z_c \geq Z_{\alpha/2}$ , then the trend of the data is considered significant; otherwise, it is not. For this study, the significance level  $\alpha$  was set as 0.05 and 0.1.

To get information about the magnitude of the trend (amount of rainfall and temperature), we used the Sen's slope estimator proposed by Sen and Theil [41,42], and it was calculated as the median of all slopes (Equation (5)):

$$\beta = \text{Median}\left(\frac{X_i - X_j}{i - j}\right), \forall j < i \quad (5)$$

This analysis was performed using R-studio with the Kendall package and Xlstat 2018 (Addinsoft).

### 2.3.2. Continuous Wavelet Transform

CWT was used to study the periodic structure of the annual average rainfall often hidden in the time series [34,43]. For a given time series  $x_t$ , CWT is a convolution of  $x_t$  with a scaled and translated mother wavelet. In this study, the complex "Morlet" wavelet [44] function was used because of its better time-frequency localization when compared to other commonly used wavelets, such as the Mexican Hat and the Daubechies wavelets [26] as Equation (6):

$$\Psi_0(\eta) = \pi^{-\frac{1}{4}} e^{-i\omega_0 n} e^{-n^2/2} \quad (6)$$

The wavelet transform  $W_n(S)$  is the inner product (or convolution) of the wavelet function with the original time series as Equation (7):

$$W_n(S) = \sum_{n'=0}^{N-1} X_{n'} * \Psi^* \left[ \frac{(n' - n)\delta t}{S} \right] \quad (7)$$

where  $n$  is the localized time-series,  $n'$  is the time variable,  $s$  is the wavelet scale,  $\delta t$  is the sampling period,  $N$  is the number of points in the time series, and the asterisk (\*) indicates the complex conjugate.

The result of the CWT is displayed by plotting the wavelet power spectrum  $|W_n(S)|^2$  obtained. In our study, the wavelet transform was performed using Matlab R2016a (MathWorks) software with the code developed elsewhere [25].

### 2.3.3. Elevation Dependence of Temperature Trends and Rainfall Trends

Polynomial regression was used to assess the elevation dependence of temperature trends and rainfall trends. Even though some studies have already proved the linear relationship between these variables [19,20,45], the result of the study of [46,47] found that the relationship existing between rainfall, temperature, and altitude does not always stand linear, especially for a tropical island [48]. Considering that linear equations are not well suited to depicting the relationships of rainfall with

topography and temperature, we used a non-linear regression (Equation (8)) and for the relationship between rainfall temperature and elevation, we used (Equation (9)):

$$\Delta Y_i = \beta_0 + \beta_1 Z_i + \beta_2 Z_i^2 + \dots + \beta_n Z_i^n \quad (8)$$

$$\Delta Y_i = \beta_{00} + \beta_{10} X_i + \beta_{01} Z_i + \beta_{20} X_i^2 + \beta_{02} Z_i^2 + \dots + \beta_{n0} X_i^n + \beta_{0n} Z_i^n + \beta_{nn} X_i^n Z_i^n \quad (9)$$

where the dependent variable  $\Delta Y_i$  is the trend detected in rainfall for the region  $i$ ,  $Z_i$  is the altitude of region  $i$ ,  $X_i$  is the temperature change of region  $i$ , and  $\beta_s$  are the regression coefficients. The order  $n$  of our model was determined by assessing  $R^2$  and  $p$ -value; we stopped increasing the order when it does not improve the fit of the model anymore. We began with a null model with zero-order and increased the model complexity as long as it could be justified with the physical explanation.

### 3. Results and Discussions

#### 3.1. The Warming in Madagascar

The average annual temperature of Madagascar increased by about 0.0042 °C per year since 1901. Through the preliminary analysis, we saw an abrupt change in the average annual temperature after 1990. Hence, we divided the time series into two epochs: 1901 to 1990 and 1991 to 2017. The first epoch had a significant decreasing trend (−0.0049 °C per year), while the second epoch displayed a significant increasing trend (0.02 °C per year). The decreasing trend in average annual temperature during the first epoch reflects the global cooling during the 1940s [17,49]. The study of Nematchoua et al. and Tadross et al. [15,17] suggested that the annual temperature of Madagascar in the 21st century is 0.2 °C warmer compared with the 1950s. Overall, Niang et al. [50] reported that Africa is now 0.5 °C warmer compared with the last century. The rise of annual temperature after the 1970s co-occurs simultaneously in Africa and the rest of the world [50,51]. However, similar to our findings, some African countries only experienced significant warming after the 1990s [52]. The study of Collins [53] presented that the African temperature anomalies in the late 1990s were significantly higher compared with the 1970s and 1980s. Niang et al. [50] indicated strong evidence of the influence of anthropogenic activity on warming.

The annual regional temperature trend is summarized in Figure 2. Overall, both  $T_{max}$  and  $T_{min}$  increased. For annual  $T_{max}$ , 15 out of 22 regions had a warming trend (Figure 2b) and for annual  $T_{min}$ , 19 out of 22 regions experienced a rise (Figure 2a). The highest increase in annual  $T_{max}$  and  $T_{min}$  was detected in Itasy located at 1200 m of altitude with an increase of 0.05 °C per year and 0.038 °C per year, respectively. It is worth noting that except for Vakinankaratra (altitude 1500 m), 5 out of 7 regions with an increase in annual  $T_{max}$  greater than 0.02 °C per year are located at more than 800 m and all the regions with decreasing annual  $T_{max}$  are located below 47 m of elevation (see Appendix A). In line with previous studies, this result demonstrated the enhancement rate of warming with elevation [54–56] inseparable to global warming [55]. Furthermore, we found that annual  $T_{max}$  is rapidly warming compared to annual  $T_{min}$ , which has occurred in some countries in the East Africa too [57]. Despite the difference between the magnitude of increase in annual  $T_{max}$  and  $T_{min}$ , previous studies and ours agree on the warming of both annual  $T_{min}$  and  $T_{max}$  [50,53].

Overall, seasonal analysis revealed an increase in temperature in both winter and summer despite the existence of decrease in some regions. The increase in  $T_{max}$  in summer was between 0.0009 and 0.05 °C per year and in winter it was between 0.0009 and 0.07 °C per year. The increase in  $T_{min}$  in summer and winter was between 0.003 and 0.05 °C per year and 0.005 and 0.05 °C per year, respectively, suggesting a greater warming in winter compared to summer. It is worth noting that unlike annual  $T_{max}$ , except for  $T_{max}$  in summer, the variation of  $T_{min}$  and  $T_{max}$  in both seasons did not show a correlation with the elevation (Figure 3). Despite the existence of decrease in seasonal temperature at some regions, it is evident that both seasons had warming, and the findings are in agreement with the results of previous studies [15,17]. The increase in temperature in Angola, Namibia, was also greater in

winter [58]. As a whole, our findings are in line with studies on the African continent revealing the warming of both seasons and a difference in the magnitude of increase for both seasons.

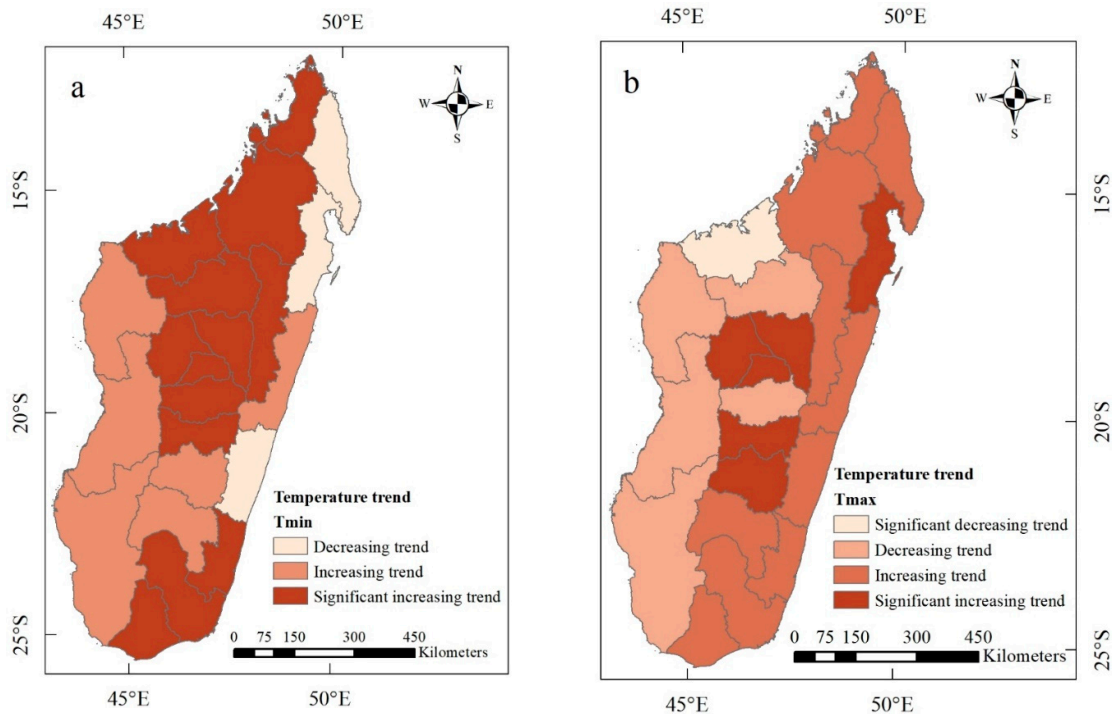


Figure 2. Annual (a) Tmin and (b) Tmax trend for each region of Madagascar.

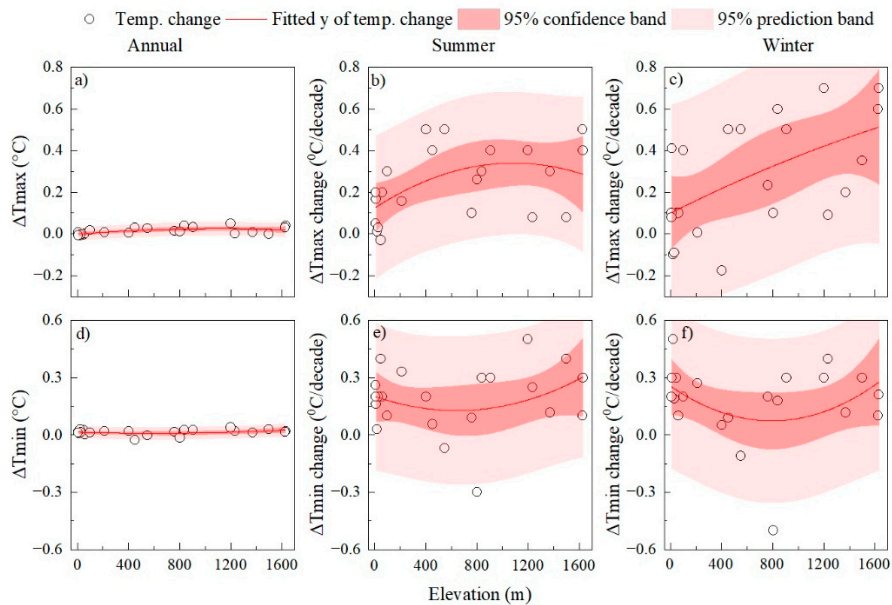
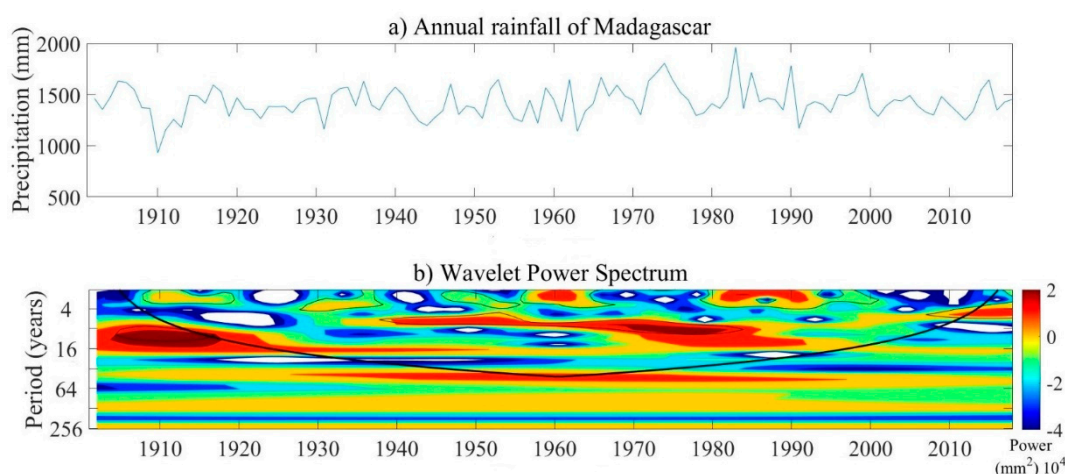


Figure 3. Trend magnitudes of (a) annual Tmax, (b) summer Tmax, (c) winter Tmax, (d) Annual Tmin (e) summer Tmin, and (f) winter Tmin according to the elevation. Open circles, dark panels, light panel and solid line indicate calculated values, 95% confidence band, 95% prediction band and best curve-fit line, respectively.

### 3.2. Changes in Annual Rainfall

#### 3.2.1. Increases in Annual Average Rainfall of Madagascar

The MK-test applied to the annual average rainfall indicated an increase of 42 mm per decade, but this change was statistically insignificant. We did not find an abrupt change in the data through the preliminary analysis. The insignificance of the rainfall changing trend was often seen in other studies in Southern Africa [59]. The annual average rainfall in Madagascar and CWT results on annual average rainfall are shown in Figure 4. The CWT revealed a 2–8 years interannual periodicity in annual average rainfall in 1910–1920, 1927–1938; 1938–1984, and 1980–1992. It is worth noting that power detected at 1 to 2 years of the band can be used to detect wet and dry years [60]. Thus, the power in the 1960s and between 1980 and 1990 indicated a wet period and explained the increasing trend in the annual average rainfall. The change in rainfall patterns in the 1980s happened across the whole African continent [59]. The periodicity found in this study accords well with the rainfall cycles in equatorial east Africa [61] and our findings are in line with other studies of African and general tropical rainfall variability [62,63].



**Figure 4.** (a) Annual average rainfall and (b) Wavelet analysis of the annual rainfall of Madagascar. The thick black contour designates the 95% confidence level against red noise. The cone of influence (COI) where edge effects might distort is shown as the U-shape line.

#### 3.2.2. Changes in regional annual rainfall of Madagascar

The annual rainfall analysis presented an increasing trend for the following regions: SAVA (10.02 mm per year), Sofia (9.27 mm per year), Betsiboka (6.42 mm per year), Analamanga (0.71 mm per year), Bongolava (10.01 mm per year), Itasy (13.51 mm per year), Vakinankaratra (2.05 mm per year), Amoron'i Mania (9.66 mm per year), and Ihorombe (8.97 mm per year), while a decreasing trend was noticed for the others (Figure 5). The results for Atsimo Antsinanana ( $p = 0.09$ ), Ihorombe ( $p = 0.05$ ), and Itasy ( $p = 0.06$ ) were statistically significant. All of the regions with an increasing trend of annual rainfall were located above 400 m altitude and at the center of Madagascar. This finding indicated a relative correlation between the annual rainfall and the altitude. Almost all regions on the coast side indicated a decreasing rainfall, except SAVA, while regions located in the central part of the island, except Matsiatra Ambony, showed an increasing trend (Figure 5). The study of Zeng et al. [22] and Yu et al. [21] explained the same results and their findings agree with ours. The highest rise of rainfall detected was for Itasy, the region in the central part of the island with 13.51 mm per year. According to the temperature analysis, Itasy was the region with the highest increase in annual temperature, suggesting the existence of the warmer-becomes-wetter phenomena. Indeed, the water-holding capacity of the atmosphere increases by about 7% change for a 1 °C increase in temperature [64]. The highest loss of annual rainfall was noticed at Atsimo Antsinanana located on the East coast,

where rainfall has decreased about 23.8 mm per year. However, Atsimo Atsinanana was not a region with the lowest warming or a decreasing annual temperature, so it implied the influence of elevation on the change of rainfall. The lowest change was noticed at Atsimo Andrefana, a region located on the South coast with only 0.1 mm per year of decrease.

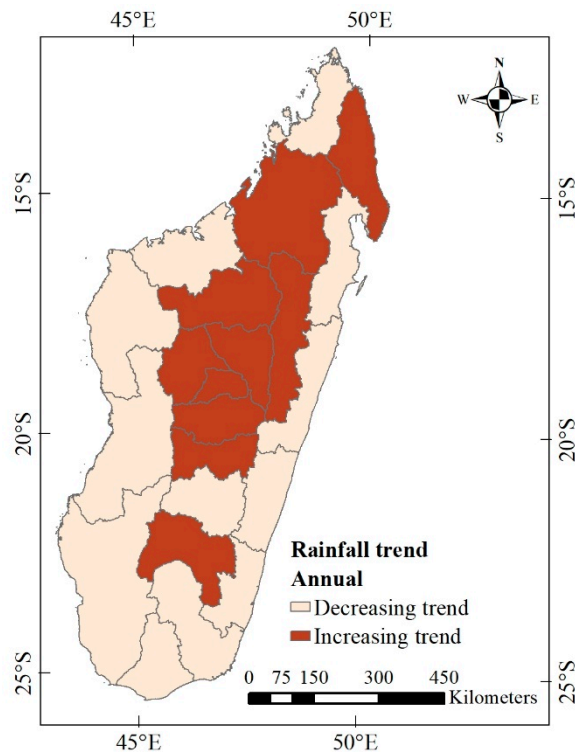


**Figure 5.** Results of the M-K test for annual rainfall in each region of Madagascar.

### 3.2.3. Correlation between Elevation and Annual Rainfall Variation

According to the polynomial regression results, the annual rainfall and elevation have a strong co-relationship ( $R^2 = 0.49$ ,  $p < 0.05$ ) (Figure 6a). We found that along the climatological gradient, the annual rainfall increased in the wet region (mean annual rainfall: 1000–2000 mm per year), revealing the phenomenon of the “wet becomes wetter”. Yet, we also noticed that the wettest region (mean annual rainfall more than 2000 mm per year) located at a lower altitude was subject to a decrease in rainfall, suggesting the influence of altitude on the change in rainfall. Thus, we classified the annual rainfall trend of Madagascar according to altitude (Figure 7). The two first regions are located at more than 850 m and beneath 200 m of altitude, associated with rainfall changes more than  $\pm 5$  mm per year. The third and fourth categories are the regions with a rainfall trend between  $\pm 5$  and  $\pm 0.5$  mm per year, regions between 200 m to 450 m of elevation had a decreasing amount of rainfall, and those located between 500 m to 850 m had an increasing amount of rainfall. The last category is the region located between 450 and 500 m altitude, characterized by the smallest change observed between  $-0.5$  and  $+0.5$  mm per year. It showed that the region in the central part of the country experienced a rise while the regions in the coast side experienced a declining annual rainfall. A similar result was found by Yao et al. and Zeng et al. [20,22] with a positive correlation between rainfall and elevation. This result is important for planning climate-related activities such as rain-fed and irrigation agriculture and can be scaled up to other studies in the African continent [39]. Furthermore, even if annual rainfall is not directly correlated with soil erosion and infiltration [65], this change in annual rainfall according to the elevation will have a different effect on soil and hydrology along the climatological gradient and altitude, as reported by [66].

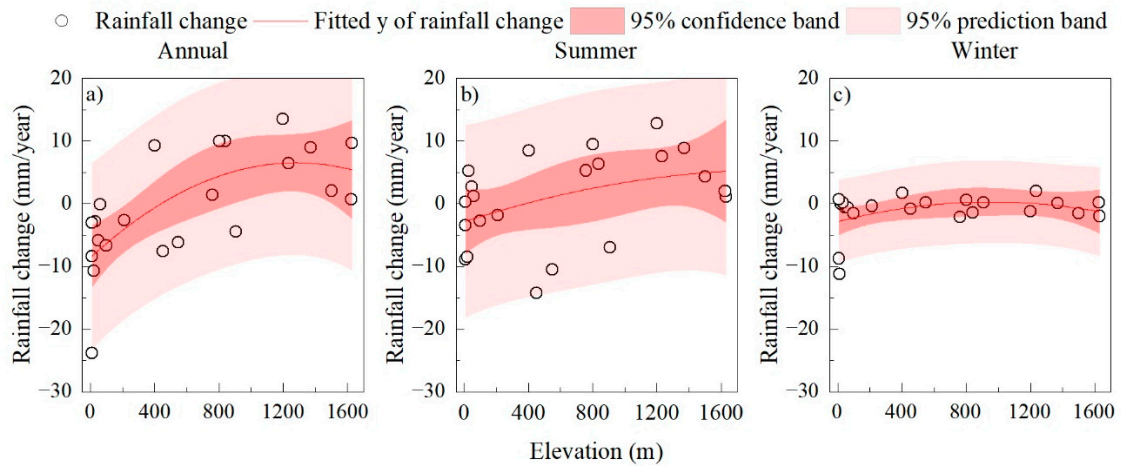


**Figure 6.** Trend magnitude of (a) annual rainfall, (b) summer rainfall and (c) winter rainfall according to elevation. Open circles, dark panels, light panel, and solid line indicate calculated values, 95% confidence band, 95% prediction band, and best curve-fit line, respectively.

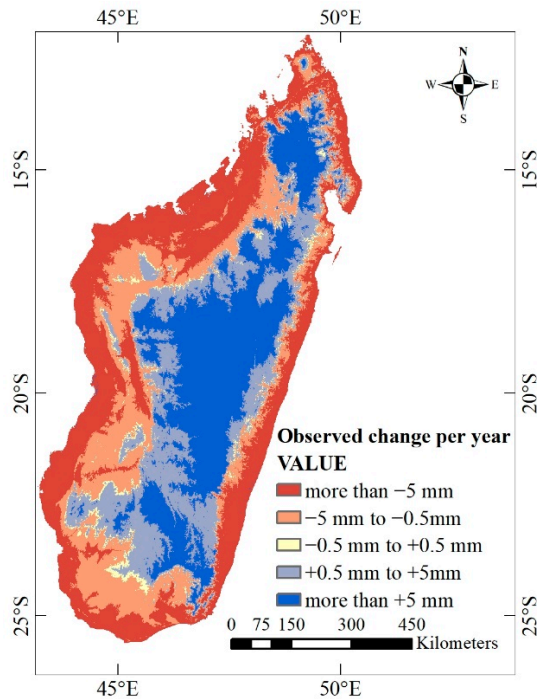


**Figure 7.** Observed change of rainfall according to elevation in Madagascar.

3.3. The Phenomenon of Wet becomes Wetter and the Warmer Becomes Wetter

3.3.1. Changes in Regional Seasonal Rainfall

The analysis of the seasonal rainfall revealed that during summer, except for the regions of Ihorombe (8.91 mm per year), Menabe (0.32 mm per year), and Sofia (8.48 mm per year) with significant increasing rainfall, and Matsiatra Ambony (−6.97 mm per year) with decreasing rainfall, the other regions had a non-significant change in rainfall (Figure 8a). In winter, only two regions had a significant trend, an increasing one for Menabe (0.66 mm per year) in the West and a decreasing one for Atsimo Antsinanana (−11 mm per year) in the East (Figure 8b).

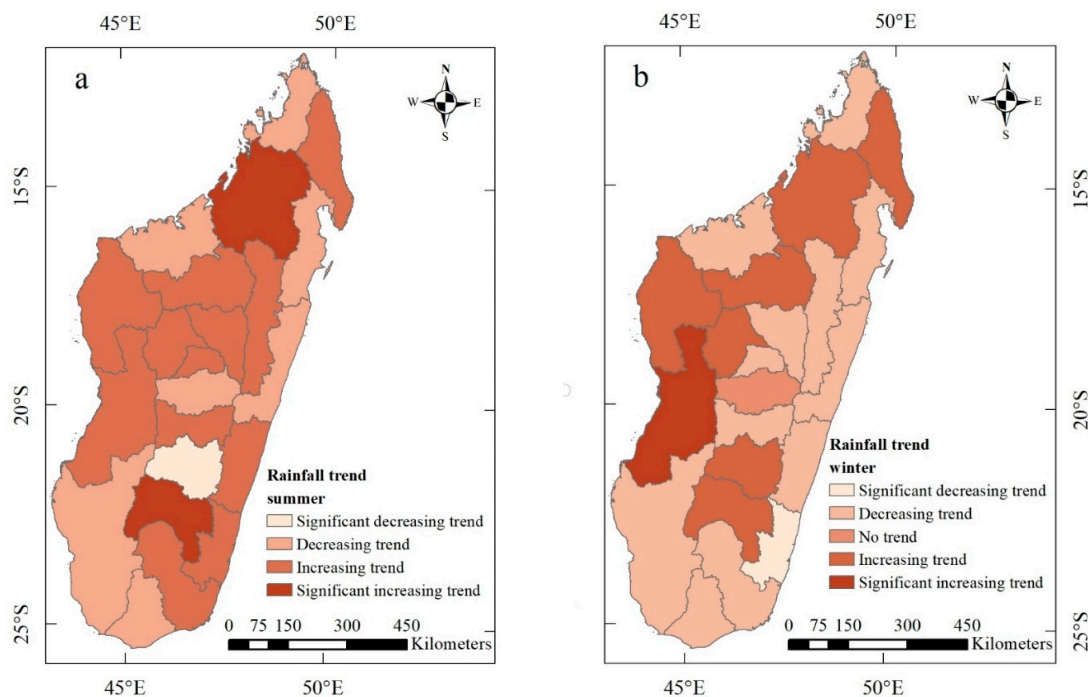


**Figure 8.** (a) Summer and (b) winter rainfall trend for each region in Madagascar.

In summer, 14 out of 22 of the regions presented an increasing rainfall, and during winter, this rate was inverted with 13 regions out of 22 with a decreasing rainfall. In summer, 10 out of 14 regions with increasing rainfall are located above 400 m altitude. The highest increase in rainfall was recorded in Itasy with 12.83 mm per year suggesting the influence of temperature and elevation over the rainfall pattern as the region is among the highest increase of summer temperature. The summer rainfall indicated a change according to the elevation—it decreased for the area below 400 m and increased for the area above 400 m (Figure 6b).

In winter, the rainfall patterns mainly declined, and the highest decrease was detected in Atsimo Atsinanana with  $-11.23$  mm per year. These findings are in line with a study by Tadross et al. [17], who also detected a reduction of rainfall of Madagascar in winter. However, the influence of warming and elevation on rainfall in winter was not evident. Similar results were reported by Zeng et al. [22], who found a different influence of elevation on seasonal rainfall and different fluctuations in trend with elevation.

This finding suggested the existence of wet-becomes-wetter and warmer-becomes-wetter in Madagascar. Because of the human-induced climate change, scientists have been projecting that rainfall patterns will shift. Hence, there will be a seasonally dependent response in rainfall patterns to global warming [67]. As summer gets warmer and is a wet season in Madagascar, it gets more rainfall. A declining rainfall trend in some African countries for both seasons was reported [58]. However, they also discovered different seasonal rainfall variations. In Kenya and Tanzania, for example, rainfall declined in winter and increased during the summer, similar to the findings of this study.

### 3.3.2. Correlation between Rainfall, Temperature, and Elevation

We used the multivariate polynomial regression to understand rainfall variation according to the increase in temperature and elevation. We added other variables (such as relative humidity, wind, sea surface temperature, soil moisture) that might influence rainfall to the model [59,68] but only temperature and elevation were significant. Furthermore, adding them to the model did not improve the fit of the model. To avoid multicollinearity, we used the average temperature trend (average of  $\Delta T_{max}$  and  $\Delta T_{min}$ ). The model indicated that annual warming and elevation influenced the annual rainfall. The model that best fits our data is a model with second-order temperature and first-order

elevation ( $R^2 = 0.6, p < 0.05$ ). Figure 9 is a contour plot of the relationship between rainfall variation, average annual temperature variation, and elevation. The maximum increase in rainfall was associated with the highest temperature rise and highest elevation (upper left and right in Figure 9). Beyond an increase in temperature of  $0.035\text{ }^\circ\text{C}$  per year, the rainfall was uniformly rising at all elevations. The increase in temperature between  $0.035$  to  $0.04\text{ }^\circ\text{C}$  per year corresponded to an increase in rainfall of  $+5\text{ mm}$  per year to  $+10\text{ mm}$  per year. Warming of  $0.04$  to  $0.045\text{ }^\circ\text{C}$  per year corresponded to an increase in rainfall of  $+10$  to  $+15\text{ mm}$  per year. However, below  $0.03\text{ }^\circ\text{C}$  per year of warming, the increase in rainfall was important at a higher elevation and the rainfall decreased at a lower elevation [22]. Decrease in rainfall about more than  $-5\text{ mm}$  per year was observed at the region below  $200\text{ m}$  and between  $0$  and  $-5\text{ mm}$  per year for the region below  $800\text{ m}$  for  $0.02\text{ }^\circ\text{C}$  per year warming. The increase in temperature leads to an increase in rainfall and it suggested a direct influence of global warming on rainfall [64]. As a result of global warming, we found that the annual temperature in Madagascar increased along the elevation. Consequently, the higher increase in yearly temperature at higher elevation resulted in a significant increase in water vapor at high altitudes and a subsequent increase in annual rainfall for the region at a higher altitude [20]. Nevertheless, an increase in annual temperature (more than  $0.03\text{ }^\circ\text{C}$ ) increased water vapor regardless of elevation; hence, the increase in annual rainfall at any altitude. The change in rainfall discovered in this study is the result of combined complex topographical and warming effects, leading to a change in hydrology. The change in rainfall is expected to result in flooding at a higher altitude and drought at a lower altitude [69].

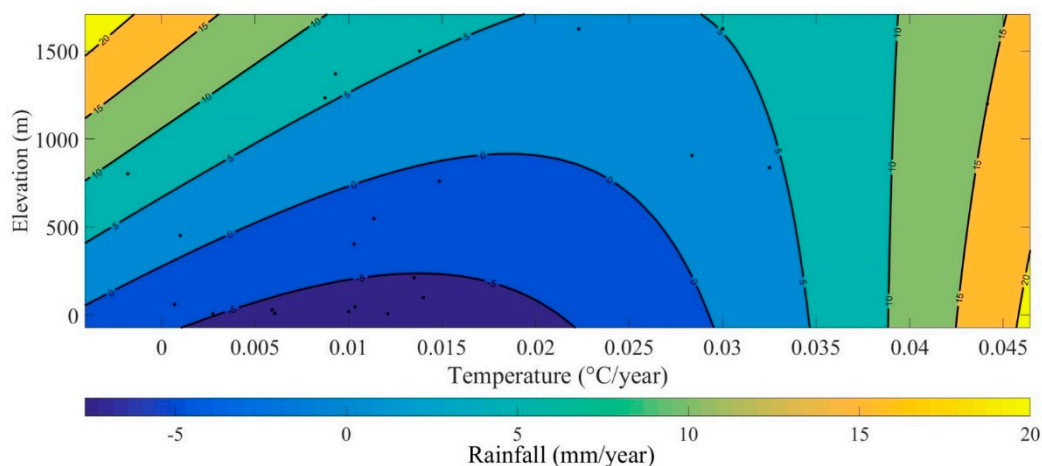


**Figure 9.** Contour plot of rainfall variation, temperature, and elevation.

Our findings provide relevant information to understand climate change and global warming for a better understanding of the earth's climate. This research provides spatial and temporal variability of rainfall and temperature in a tropical climate where hydroclimatic study is crucial but still lacking. It is worth noting that we did not find a significant influence of elevation and seasonal warming on seasonal rainfall. Thus, deep investigation into the influence of seasonal warming on seasonal rainfall needs to be done in future works.

#### 4. Conclusions

The impact of global warming on rainfall was dependent on elevation. Under warming of temperature in Madagascar, the increase in rainfall was prominent at a higher elevation than lower elevation. However, with an increase in temperature more than  $0.03\text{ }^\circ\text{C}$  per year, rainfall increased both in lower and higher elevated regions. Furthermore, the phenomena of “wet-becomes-wetter” and “warmer-becomes-wetter” is existent in Madagascar with an important increase in rainfall in summer compared to winter. The knowledge of elevation dependence of the impacts of warming on rainfall is important for water resource management and climate change adaptation strategies at

a local level. Our research provides relevant information for research on climate change and global warming, which helps for a better understanding of the earth's climate. Our findings can be used as a tool for policymakers or a basis for climate simulation in other regions with similar climates as Madagascar. While for regions with a different climate than our study area, our results can be used to prove that the impact of global warming on rainfall is unevenly distributed. The influence of seasonal warming on seasonal rainfall was not evident in this study. Thus, we suggest future works to deepen the understanding of the phenomenon of “wet-becomes-wetter” and “warmer-becomes-wetter” in another tropical region through high-resolution climate modeling.

**Author Contributions:** Conceptualization, M.F.R.T. and J.Z.; Methodology, M.F.R.T., J.Z., and T.M.A.; Validation, M.F.R.T., J.Z., T.M.A., and J.C.; Formal Analysis, J.Z. and T.M.A.; Resources, M.F.R.T. and J.Z.; Writing—Original Draft Preparation, M.F.R.T., T.M.A., and J.Z.; Writing—Review & Editing, M.F.R.T., T.M.A., and J.Z.; Visualization, T.M.A., J.Z., and J.C.; Supervision, J.Z., T.M.A., and J.C.; Funding Acquisition, J.Z. All authors have read and agreed to the published version of the manuscript.

**Funding:** This work was funded by the National Natural Science Foundation of China (No. 51878093), National Key R&D Program of China (2018YFB2101001-03), and Chongqing Technology Innovation and Application Demonstration Special Project—Key Research And Development Projects Related to People's Livelihood (cstc2018jcsx-mszdX0087, cstc2018jszx-336 zdyfxmX0009).

**Conflicts of Interest:** The authors declare no conflict of interest.

## Appendix A

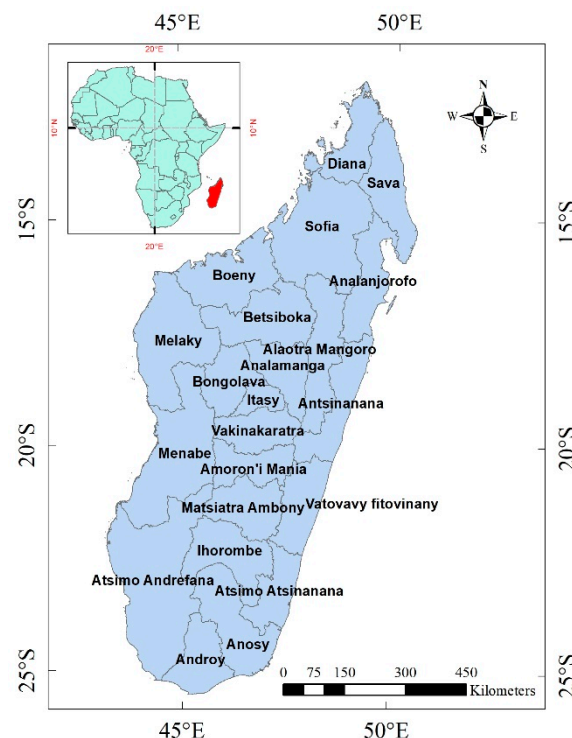


**Figure A1.** Localization of the study area with the name of regions used in this study.

## References

1. NASA. Available online: <https://climate.nasa.gov/vital-signs/global-temperature/> (accessed on 19 July 2020).
2. Ahmadalipour, A.; Moradkhani, H.; Castelletti, A.; Magliocca, N. Future drought risk in Africa: Integrating vulnerability, climate change, and population growth. *Sci. Total Environ.* **2019**, *662*, 672–686. [[CrossRef](#)] [[PubMed](#)]

3. Fujihara, Y.; Tanaka, K.; Watanabe, T.; Nagano, T.; Kojiri, T. Assessing the impacts of climate change on the water resources of the Seyhan River Basin in Turkey: Use of dynamically downscaled data for hydrologic simulations. *J. Hydrol.* **2008**, *353*, 33–48. [[CrossRef](#)]
4. IPCC. *Climate Change 2014: Synthesis Report. Contribution of Working Groups I, II and III to the Fifth Assessment Report of the Intergovernmental Panel on Climate Change*; IPCC: Geneva, Switzerland, 2014; p. 151.
5. Zhu, Y.; Lin, Z.; Wang, J.; Zhao, Y.; He, F. Impacts of Climate Changes on Water Resources in Yellow River Basin, China. *Procedia Eng.* **2016**, *154*, 687–695. [[CrossRef](#)]
6. Huang, Y.; Cai, J.; Yin, H.; Cai, M. Correlation of precipitation to temperature variation in the Huanghe River (Yellow River) basin during 1957–2006. *J. Hydrol.* **2009**, *372*, 1–8. [[CrossRef](#)]
7. Yang, P.; Xia, J.; Zhang, Y.; Hong, S. Temporal and spatial variations of precipitation in Northwest China during 1960–2013. *Atmos. Res.* **2017**, *183*, 283–295. [[CrossRef](#)]
8. Ahmadelipour, A.; Moradkhani, H. Multi-dimensional assessment of drought vulnerability in Africa: 1960–2100. *Sci. Total Environ.* **2018**, *644*, 520–535. [[CrossRef](#)]
9. Sannigrahi, S.; Zhang, Q.; Joshi, P.; Sutton, P.C.; Keesstra, S.; Roy, P.; Pilla, F.; Basu, B.; Wang, Y.; Jha, S.; et al. Examining effects of climate change and land use dynamic on biophysical and economic values of ecosystem services of a natural reserve region. *J. Clean. Prod.* **2020**, *257*, 120424. [[CrossRef](#)]
10. Chen, Y.; Liu, A.; Cheng, X. Quantifying economic impacts of climate change under nine future emission scenarios within CMIP6. *Sci. Total Environ.* **2020**, *703*, 134950. [[CrossRef](#)]
11. Epule, T.E.; Ford, J.D.; Lwasa, S. Projections of maize yield vulnerability to droughts and adaptation options in Uganda. *Land Use Policy* **2017**, *65*, 154–163. [[CrossRef](#)]
12. Morishima, W.; Akasaka, I. Seasonal trends of rainfall and surface temperature over southern Africa. *Afr. Study Monogr.* **2010**, *40*, 67–76.
13. Vera, J.F.R.; Mera, Y.E.Z.; Pérez-Martin, M. Adapting water resources systems to climate change in tropical areas: Ecuadorian coast. *Sci. Total Environ.* **2020**, *703*, 135554. [[CrossRef](#)] [[PubMed](#)]
14. Muluneh, A.; Stroosnijder, L.; Keesstra, S.; Biazin, B. Adapting to climate change for food security in the Rift Valley dry lands of Ethiopia: Supplemental irrigation, plant density and sowing date. *J. Agric. Sci.* **2017**, *155*, 703–724. [[CrossRef](#)]
15. Nematchoua, M.K.; Ricciardi, P.; Orosa, J.A.; Buratti, C. A detailed study of climate change and some vulnerabilities in Indian Ocean: A case of Madagascar Island. *Sustain. Cities Soc.* **2018**, *41*, 886–898. [[CrossRef](#)]
16. Joly, F. Le climat de Madagascar. *L'inf. Geogr.* **1941**, *5*, 76–80. [[CrossRef](#)]
17. Tadross, M.; Randriamarolaza, L.; Yip, Z.K. *Climate Change in Madagascar; Recent past and future*; World Bank: Washington, DC, USA, 2008; pp. 1–18.
18. Middletown, J.; McMaster, D. Africa. Available online: <https://www.britannica.com/place/Africa> (accessed on 28 May 2020).
19. Xu, F.; Liu, H.; Peng, H.; Niu, C.; Liu, J. Temperature and precipitation trends and their links with elevation in the Hengduan Mountain region, China. *Clim. Res.* **2018**, *75*, 163–180. [[CrossRef](#)]
20. Yao, J.; Yang, Q.; Mao, W.; Zhao, Y.; Xu, X. Precipitation trend–Elevation relationship in arid regions of the China. *Glob. Planet. Chang.* **2016**, *143*, 1–9. [[CrossRef](#)]
21. Yu, H.; Wang, L.; Yang, R.; Yang, M.; Gao, R. Temporal and spatial variation of precipitation in the Hengduan Mountains region in China and its relationship with elevation and latitude. *Atmos. Res.* **2018**, *213*, 1–16. [[CrossRef](#)]
22. Zeng, W.; Yu, Z.; Wu, S.; Qin, J. Changes in annual, seasonal and monthly precipitation events and their link with elevation in Sichuan province, China. *Int. J. Clim.* **2015**, *36*, 2303–2322. [[CrossRef](#)]
23. Qing, Y.; Zhu-Guo, M.; Liang, C. A Preliminary Analysis of the Relationship between Precipitation Variation Trends and Altitude in China. *Atmos. Ocean. Sci. Lett.* **2011**, *4*, 41–46. [[CrossRef](#)]
24. Rashid, M.; Beecham, S.; Chowdhury, R.K. Assessment of trends in point rainfall using Continuous Wavelet Transforms. *Adv. Water Resour.* **2015**, *82*, 1–15. [[CrossRef](#)]
25. Torrence, C.; Compo, G. A practical guide to Wavelet Analysis. *J. Am. Meteorol. Soc.* **1998**, *79*, 61–78. [[CrossRef](#)]
26. Roushangar, K.; Alizadeh, F.; Adamowski, J.F. Exploring the effects of climatic variables on monthly precipitation variation using a continuous wavelet-based multiscale entropy approach. *Environ. Res.* **2018**, *165*, 176–192. [[CrossRef](#)] [[PubMed](#)]

27. Kendall, M.G. *Rank Correlation Methods*, 5th ed.; Griffin, C., Ed.; Oxford University Press: London, UK, 1975; ISBN 978-0195208375.
28. Mann, H.B. Nonparametric tests against trend. *Econometrica* **1945**, *13*, 245–259. [[CrossRef](#)]
29. Animashaun, I.; Oguntunde, P.; Akinwumiju, A.; Olubanjo, O. Rainfall Analysis over the Niger Central Hydrological Area, Nigeria: Variability, Trend, and Change point detection. *Sci. Afr.* **2020**, *8*, e00419. [[CrossRef](#)]
30. Asare-Nuamah, P.; Botchway, E. Understanding climate variability and change: Analysis of temperature and rainfall across agroecological zones in Ghana. *Heliyon* **2019**, *5*, e02654. [[CrossRef](#)]
31. Valipour, M.; Bateni, S.; Sefidkouhi, M.A.G.; Raeini-Sarjaz, M.; Singh, V.P. Complexity of Forces Driving Trend of Reference Evapotranspiration and Signals of Climate Change. *Atmosphere* **2020**, *11*, 1081. [[CrossRef](#)]
32. Gentilucci, M.; Bisci, C.; Burt, P.; Fazzini, M.; Vaccaro, C. Interpolation of Rainfall through Polynomial Regression in the Marche Region (Central Italy). In *Geospatial Technologies for All; Lecture Notes in Geoinformation and Cartography*, Mansourian, A., Pilesjö, P., Harrie, L., van Lammeren, R., Eds.; Springer International Publishing: Cham, Switzerland, 2018; pp. 55–73.
33. Tattersall, I.; Sussman, R.W. Notes on Topography, Climate, and Vegetation of Madagascar. In *Lemur Biology*; Tattersall, I., Sussman, R.W., Eds.; Springer: Boston, MA, USA, 1975; pp. 13–21.
34. Chu, H.; Wei, J.; Qiu, J.; Li, Q.; Wang, G. Identification of the impact of climate change and human activities on rainfall-runoff relationship variation in the Three-River Headwaters region. *Ecol. Indic.* **2019**, *106*, 105516. [[CrossRef](#)]
35. Güçlü, Y.S. Multiple Şen-innovative trend analyses and partial Mann-Kendall test. *J. Hydrol.* **2018**, *566*, 685–704. [[CrossRef](#)]
36. Joshi, N.; Gupta, D.; Suryavanshi, S.; Adamowski, J.F.; Madramootoo, C.A. Analysis of trends and dominant periodicities in drought variables in India: A wavelet transform based approach. *Atmos. Res.* **2016**, *182*, 200–220. [[CrossRef](#)]
37. Mullick, R.A.; Nur, R.M.; Alam, J.; Islam, K.A. Observed trends in temperature and rainfall in Bangladesh using pre-whitening approach. *Glob. Planet. Chang.* **2019**, *172*, 104–113. [[CrossRef](#)]
38. Samarakoon, S.; Dharmagunawardhane, H.; Kularatne, T. Analysis of rainfall trend using mann-kendall test and the sen's slope estimator: A case study in Matale district in Sri Lanka. *Int. J. Agric. Environ. Res.* **2017**, *6*, 131–138.
39. Umar, D.; Ramli, M.; Aris, A.Z.; Jamil, N.R.; Aderemi, A.A. Evidence of climate variability from rainfall and temperature fluctuations in semi-arid region of the tropics. *Atmos. Res.* **2019**, *224*, 52–64. [[CrossRef](#)]
40. Yin, Y.; Xu, C.; Chen, H.; Li, L.; Xu, H.; Li, H.; Jain, S.K. Trend and concentration characteristics of precipitation and related climatic teleconnections from 1982 to 2010 in the Beas River basin, India. *Glob. Planet. Chang.* **2016**, *145*, 116–129. [[CrossRef](#)]
41. Sen, P.K. Estimates of the regression coefficient based on Kendall's Tau. *J. Am. Stat. Assoc.* **1968**, *63*, 1379–1389. [[CrossRef](#)]
42. Theil, H. A rank-invariant method of linear and polynomial regression analysis. In *Henri Theil's Contributions to Economics and Econometrics*; Springer: Dordrecht, The Netherlands, 1992; pp. 345–381.
43. Santos, C.A.G.; Ideiao, S.M.A. *Application of the Wavelet Transform for Analysis of Precipitation and Runoff 439 Time Series*; IAHS Publ.: Wallington, UK, 2006; p. 303.
44. Lau, K.M.; Weng, H. Climate signal detection using wavelet transform: How to make a time series sing. *Bull. Am. Meteorol. Soc.* **1995**, *76*, 32391–32402. [[CrossRef](#)]
45. Sokol, Z.; Bližňák, V. Areal distribution and precipitation–altitude relationship of heavy short-term precipitation in the Czech Republic in the warm part of the year. *Atmos. Res.* **2009**, *94*, 652–662. [[CrossRef](#)]
46. Dahri, Z.H.; Ludwig, F.; Moors, E.; Ahmad, B.; Khan, A.; Kabat, P. An appraisal of precipitation distribution in the high-altitude catchments of the Indus basin. *Sci. Total Environ.* **2016**, 289–306. [[CrossRef](#)]
47. Palazzi, E.; Filippi, L.; Von Hardenberg, J. Insights into elevation-dependent warming in the Tibetan Plateau-Himalayas from CMIP5 model simulations. *Clim. Dyn.* **2017**, *48*, 3991–4008. [[CrossRef](#)]
48. Sanchez-Moreno, J.F.; Mannaerts, C.M.; Jetten, V. Influence of topography on rainfall variability in Santiago Island, Cape Verde. *Int. J. Clim.* **2013**, *34*, 1081–1097. [[CrossRef](#)]
49. Nicholson, S.E.; Nash, D.J.; Chase, B.M.; Grab, S.W.; Shanahan, T.M.; Verschuren, D.; Asrat, A.; Lézine, A.-M.; Umer, M. Temperature variability over Africa during the last 2000 years. *Holocene* **2013**, *23*, 1085–1094. [[CrossRef](#)]

50. Niang, I.; Abdrabo, M.; Essel, A.; Lennard, C.; Padgham, J.; Urquhart, P. *Africa in Climate Change 2014: Impacts, Adaptation, and Vulnerability, Part B: Regional Aspects*; Contribution of Working Group II to the Fifth Assessment Report of the Intergovernmental Panel on Climate Change; Cambridge University Press: Cambridge, UK; New York, NY, USA, 2014; pp. 1199–1295.
51. Hulme, M.; Doherty, R.; Ngara, T.; New, M.; Lister, D. African climate change: 1900–2100. *Clim. Res.* **2001**, *17*, 145–168. [[CrossRef](#)]
52. Ongoma, V.; Chen, H. Temporal and spatial variability of temperature and precipitation over East Africa from 1951 to 2010. *Theor. Appl. Clim.* **2017**, *129*, 131–144. [[CrossRef](#)]
53. Collins, J.M. Temperature Variability over Africa. *J. Clim.* **2011**, *24*, 3649–3666. [[CrossRef](#)]
54. Mountain Research Initiative EDW Working Group; Pepin, N.; Bradley, R.S.; Diaz, H.F.; Baraer, M.; Caceres, E.B.; Forsythe, N.; Fowler, H.J.; Greenwood, G.; Hashmi, M.Z.; et al. Elevation-dependent warming in mountain regions of the world. *Nat. Clim. Chang.* **2015**, *5*, 424–430. [[CrossRef](#)]
55. Wang, Q.; Fan, X.; Wang, M.-B. Recent warming amplification over high elevation regions across the globe. *Clim. Dyn.* **2013**, *43*, 87–101. [[CrossRef](#)]
56. Fan, Z.-X.; Bräuning, A.; Thomas, A.; Li, J.-B.; Cao, K.-F. Spatial and temporal temperature trends on the Yunnan Plateau (Southwest China) during 1961–2004. *Int. J. Clim.* **2010**, *31*, 2078–2090. [[CrossRef](#)]
57. Gebrechorkos, S.H.; Hülsmann, S.; Bernhofer, C. Long-term trends in rainfall and temperature using high-resolution climate datasets in East Africa. *Sci. Rep.* **2019**, *9*, 1–9. [[CrossRef](#)]
58. Thomas, N.; Nigam, S. Twentieth-Century Climate Change over Africa: Seasonal Hydroclimate Trends and Sahara Desert Expansion. *J. Clim.* **2018**, *31*, 3349–3370. [[CrossRef](#)]
59. Nicholson, S.E.; Funk, C.; Fink, A.H. Rainfall over the African continent from the 19th through the 21st century. *Glob. Planet. Chang.* **2018**, *165*, 114–127. [[CrossRef](#)]
60. Santos, C.A.G.; Da Silva, R.M.; Akrami, S.A. Rainfall Analysis in Klang River Basin Using Continuous Wavelet Transform. *J. Urban Environ. Eng.* **2016**, *10*, 3–10. [[CrossRef](#)]
61. Janowiak, J.E. An Investigation of Interannual Rainfall Variability in Africa. *J. Clim.* **1988**, *1*, 240–255. [[CrossRef](#)]
62. Nicholson, S.E.; Entekhabi, D. The quasi-periodic behavior of rainfall variability in Africa and its relationship to the southern oscillation. *Theor. Appl. Clim.* **1986**, *34*, 311–348. [[CrossRef](#)]
63. Niedzielski, T. El Niño/Southern Oscillation and Selected Environmental Consequences. In *Machine Learning in Geosciences*; Elsevier: Amsterdam, The Netherlands, 2014; Volume 55, pp. 77–122.
64. Trenberth, K. Changes in precipitation with climate change. *Clim. Res.* **2011**, *47*, 123–138. [[CrossRef](#)]
65. Cerdà, A. Relationships between climate and soil hydrological and erosional characteristics along climatic gradients in Mediterranean limestone areas. *Geomorphology* **1998**, *25*, 123–134. [[CrossRef](#)]
66. Cerdà, A. Effect of climate on surface flow along a climatological gradient in Israel: A field rainfall simulation approach. *J. Arid. Environ.* **1998**, *38*, 145–159. [[CrossRef](#)]
67. Putnam, A.; Broecker, W.S. Human-induced changes in the distribution of rainfall. *Sci. Adv.* **2017**, *3*, e1600871. [[CrossRef](#)]
68. Ambrosino, C.; Chandler, R.E.; Todd, M.C. Southern African Monthly Rainfall Variability: An Analysis Based on Generalized Linear Models. *J. Clim.* **2011**, *24*, 4600–4617. [[CrossRef](#)]
69. Keesstra, S.; Nunes, J.P.; Saco, P.M.; Parsons, A.J.; Poeppel, R.; Masselink, R.; Cerda, A. The way forward: Can connectivity be useful to design better measuring and modelling schemes for water and sediment dynamics? *Sci. Total Environ.* **2018**, *644*, 1557–1572. [[CrossRef](#)]

**Publisher’s Note:** MDPI stays neutral with regard to jurisdictional claims in published maps and institutional affiliations.



© 2020 by the authors. Licensee MDPI, Basel, Switzerland. This article is an open access article distributed under the terms and conditions of the Creative Commons Attribution (CC BY) license (<http://creativecommons.org/licenses/by/4.0/>).